Environmental Science: Atmospheres

ROYAL SOCIETY OF CHEMISTRY

PAPER

View Article Online
View Journal | View Issue

Cite this: *Environ. Sci.: Atmos.*, 2024, **4**, 1229

Ozone formation potential related to the release of volatile organic compounds (VOCs) and nitrogen oxide (NO_X) from a typical industrial park in the Pearl River Delta†

Taicheng An, *[ab] Jiajia Li,[ab] Qinhao Lin[ab] and Guiying Li [ab]

Ozone (O_3) pollution has been recognized as the major air pollution in the Pearl River Delta (PRD) region, South China. Understanding O_3 formation sensitive to volatile organic compound (VOC)- and nitrogen oxide (NO_X)-limited regimes is a key step for alleviating O_3 pollution. Herein, measurements of VOCs, NO_X and O_3 were simultaneously performed at multi sampling sites in an industrial park of the PRD region during June, 2020. VOCs/NO_X ratios ranged from 0.5 to 5.7, suggesting that the O_3 formation was in the VOC-limited regime in the industrial park. The estimated O_3 formation potential (OFP) of VOCs showed that alkenes and aromatic hydrocarbons from motor vehicles and industrial sources contributed to 40% and 39% of the O_3 formation, respectively, in the industrial park. However, a low O_3 level (<50 ppb) was observed in the region where high OFP values (>194 ppb) were estimated. Further analysis found that the concentration of NOx (25 ± 10 ppb) in the high O_3 region was lower than that (36 ± 6 ppb) in the low O_3 region, mostly due to the titration reaction of NO and O_3 to form NO_2, therefore leading to the consumption of O_3. This result implies that NO_X control was not conducive to the O_3 pollution in the study region. Thus, O_3 pollution control in the study region should be taken into consideration in terms of the effect of NO_X titration and control of VOC emissions.

Received 27th June 2024
Accepted 19th September 2024

DOI: 10.1039/d4ea00091a

rsc.li/esatmospheres

Environmental significance

O_3 pollution is a major air pollution in the Pearl River Delta region, China. Understanding O_3 formation sensitive to VOC- and NO_X-limited regimes is a key step for alleviating O_3 pollution. Herein, VOCs, NO_X and O_3 were simultaneously measured in a typical industrial park in this region. The ratio of VOCs to NO_X indicates that O_3 formation was in the VOC-limited regime in the industrial park. Alkenes and AHs principally from motor vehicles and industrial sources were the main potential contributors to the formation of O_3. However, no increase in O_3 was found in the abundant alkene and AH regions, mainly due to the titration reaction of NO and O_3 to form NO_2. These findings highlighted the role of NOx-titration in O_3 formation under the VOC-limited regime.

1 Introduction

Ozone (O_3) has an inverse impact on the ecosystem and human health.[1,2] High levels of O_3 can lead to a reduction in crop yields and abnormal growth of plants,[3–5] and O_3 pollution can damage the health system of humans, leading to complications such as ocular discomfort, interruption of the skin's normal barrier function and development and progression of obstructive airway diseases.[6–8] More importantly, O_3 also occurs as the by-product in the complicated photochemical reaction involving NOx and volatile organic compounds (VOCs).[9,10] The area and frequency of O_3 pollution in China showed an increasing trend in recent years.[11] The mean O_3 concentration increased from 84.3 to 95.8 μg m^{-3} from 2015 to 2018 in China,[12] especially in the Beijing–Tianjin–Hebei, Fen Wei River Plain, and Pearl River Delta (PRD) regions. The O_3 formation is highly dependent on its precursors including VOCs and NO_X.[9,10] However, non-linear relationships existed between the formation of O_3 and concentrations of VOCs and NO_X. Therefore, it is necessary to figure out the interaction between the production of O_3 and its precursors.

The formation of O_3 involves a series of complex photochemical reactions of NOx and VOCs.[13] The types and levels of VOCs and NO_X, their ratio as well as the intensity of solar radiation will influence the formation of the ground-level

[a]*Guangdong-Hong Kong-Macao Joint Laboratory for Contaminants Exposure and Health, Guangdong Key Laboratory of Environmental Catalysis and Health Risk Control, Institute of Environmental Health and Pollution Control, School of Environmental Science and Engineering, Guangdong University of Technology, Guangzhou 510006, China. E-mail: antc99@gdut.edu.cn*

[b]*Guangzhou Key Laboratory of Environmental Catalysis and Pollution Control, Key Laboratory of City Cluster Environmental Safety and Green Development of the Ministry of Education, School of Environmental Science and Engineering, Guangdong University of Technology, Guangzhou 510006, China*

† Electronic supplementary information (ESI) available. See DOI: https://doi.org/10.1039/d4ea00091a

O_3.[14,15] The O_3 formation was sensitive to its precursors in three regimes including the VOC-limited regime, the NOx-limited regime and their transition regime.[16] Therefore, the effectiveness of NOx and VOC emission control in reducing O_3 needs to be discerned so that the O_3 pollution problem can be alleviated.

VOCs and NO_X can be from natural and anthropogenic sources. The biogenic emission is an important natural source of VOCs,[17] while organic matter decomposition and lightning would generate natural NO_X.[18] However, large amounts of VOCs and NO_X produced by human activities have become the main source recently.[19] Industrial sources and vehicle exhaust are the important contributors to VOCs and NO_X emissions.[20,21]

The PRD region is one of the O_3 pollution regions in China.[22] In this region, the average O_3 concentration increased from 48 to 60 μg m^{-3} from 2006 to 2019, with an average growth rate of 0.80 μg $(m^3\ a)^{-1}$.[23] The formation of O_3 at urban sites was mainly in the VOC-limited region.[24] Moreover, industrial emission contributes to more than 40% of VOCs in this region.[25,26] To characterize VOC_S from industrial emission, the measurement of VOCs in the industrial park *via* the fixed sampling site was reported previously.[27,28] Compared to a single sampling site, observation of VOCs in industrial parks at multiple sampling sites would recognize spatial distribution characteristics and sources of VOCs.[29] Moreover, observation of VOCs at multiple sampling sites can be conducted to understand the dispersion of VOCs in an industrial park.

In this study, the observation of VOCs at 24 sampling sites was performed in an industrial park in PRD. Additionally, O_3 and NO_X were simultaneously monitored using a multi-pollutant sensor package. The objectives of this study were to (1) characterize the spatial distribution of VOCs, NO_X and O_3 in an industrial park, and (2) compare the spatial distribution of O_3 formation potential and observed O_3, and evaluate how the VOCs or NO_X are sensitive to O_3 formation.

2 Experimental section

2.1. Sampling sites

24 sampling sites are located in an industrial park in the PRD region, South China (Fig. S1†), which were decided by the principle of grid monitoring and practical situations, and the detailed description is listed in Table S1.† The industrial park consisted of more than 20 enterprises including raw material manufacturing, machinery manufacturing, chemical process, comprehensive utilization of waste resources, printing, textiles, food processing, pharmaceutical manufacturing, transportation, electronic and machine manufacturing, and research and experimental development (Fig. S1†). In addition, this industrial park is close to a main traffic road, and the traffic source therefore would be another contributor to the local air pollution. It should be noted that the industrial park is partly surrounded by a mountain, with a fully covering dense forest. Some natural VOCs (*e.g.*, isoprene) from the forest might release into the atmosphere in this industrial park. In addition, a village with approximately 15 000 residents is located in the central position of the industrial park.

2.2. Measurement of VOCs

A total of 24 sites with an interval of approximately 450 m were sampled in the industrial park area of 2.5 km × 1.6 km (Fig. S2†). The sampling period was from 10:40 to 15:00 on June 17, 2020, which the photochemical reaction was active due to enough sunlight. Wind speed was about 1 m s^{-1} and the day was sunny during the sample period. Such a low wind was unfavourable for the dispersion of VOCs from the industrial park emission. Additionally, the industrial park is partly surrounded by a mountain. The presence of the mountain in the industrial park coupled with the low wind speeds would further enhance VOC accumulation from the industrial park emissions. VOCs were sampled using 2.7 L vacuum stainless Summa canisters (ENTECH Instruments Inc., Silonite™, CA, USA) with a restrictor valve (1 L min^{-1}) above ground level of 1.5 m. Prior to sampling, each Summa canister should be filled with high purity nitrogen (99.999%), vacated and washed repeatedly for more than five times. One out of every 20 cleaned canisters needs to be filled with high purity nitrogen and placed for more than 24 h. The sample was analysed to ensure that the target compounds in the canisters could not be detected or fell below the detection limit. The sampled VOCs were analysed as soon as possible within 20 days. The collected VOC samples were detected using an Entech 7100 pre-concentrator (Entech Instruments Inc., CA, USA) and a gas chromatography-mass spectrometer (7890A GC-5975C MS, Agilent Technologies, USA) based on the USEPA TO-15 method. The detailed procedure, and qualitative and quantitative analysis methods of VOCs are provided in the ESI (Text S1†).

2.3. Measurements of O_3 and NO_X

O_3 and NO_X were monitored using a multipollutant sensor package.[30] O_3 (OX-B431), NO (NO-B4) and NO_2 (NO_2-B42) sensors were commercially obtained from Alphasense Ltd (Essex, UK). All the gas sensors were calibrated completely with standard gases.[30] NO standard gas was from Shenkai Gases Tech. Ltd (Shanghai, China), O_3 standard gas was generated *via* an O_3 generator (Ozone Primary Standard, Model 49i-PS, Thermo Fisher Scientific Inc., USA) and NO_2 was produced from the reaction between NO and O_3. After calibration, the sensors were compared with field observation instruments including a UV photometric O_3 analyser (Model49C, Thermo Electron Corporation, USA) and a NO–NO_2–NO_X monitor (Model 42i, Thermo Scientific, USA), which were applied to a monitoring test together. The detailed calibration processes were described previously.[30]

2.4. Ozone formation potential (OFP)

OFP was used to evaluate the contribution of VOCs to O_3 formation in the atmospheric photochemical reaction.[22] Taking into account the reactivity of VOCs and their concentrations in the atmosphere, the Maximum Incremental Activity (MIR) method was used to calculate the contribution of VOCs to O_3 generation in near-ground level.[31] The OFP can be expressed as:

$$\mathrm{OFP}(i) = \mathrm{Conc}(i) \times \mathrm{MIR\ coefficient}(i)$$

where Conc(i) is the concentration of compound i in the atmosphere (ppb: parts per billion by volume). MIR coefficient(i) is the MIR of compound i, which is updated previously.[32] The values of MIR are summarized in Table S2.† A total of 70 VOC species contributed to the OFP in this study.

2.5. Observation-based chemical box model

An observation-based model (OBM) combined with the master chemical mechanism simulation online (AtChem Online, https://www.atchem.york.ac.uk/, Version 2.0) was used to explore the contribution of VOCs or NO_X to O_3 formation. Averaged air pollutants (O_3, NO, NO_2, and VOCs) and meteorological parameters (temperature, pressure, relative humidity) and boundary were input into the OBM-AtChem Online as constraints. The model was run at 00:00 local time as the initial time. Relative incremental reactivity (RIR) was an indicator to diagnose the sensitivity of O_3 reduction to its precursors NO_X or O_3. The RIR can be expressed as:

$$\mathrm{RIR} = \frac{\Delta P(O_3)/P(O_3)}{\Delta X/X}$$

Here, $\Delta P(O_3)/P(O_3)$ represents differences in the O_3 production rate (Text S2†), which was calculated in the OBM-AtChem Online. $\Delta X/X$ refers to differences in precursor concentrations, and the value was 20%.

3 Results and discussion

3.1. Characteristics of VOCs

The spatial distribution of the concentrations of total VOCs (TVOCs) at 24 sampling sites in the industrial park is shown in Fig. 1a. TVOCs ranged from 13 to 120 ppb with an average level of 41 ± 24 ppb (mean ± standard deviation) in the industrial park (Fig. S3†). High values (>54 ppb) can be found in the northwestern, southwestern and southeastern areas, while low values (<33 ppb) were observed in the central region. Low TVOCs in the central region may be mostly attributed to no industrialized source of VOCs (a village situated there). Table S3† lists the TVOCs, species number and top 10 species in the industrial park, urban, suburban and rural regions of the PRD region compared with that in this study. The mean TVOCs in this study were similar to the levels (35–89 ppb) in the urban area,[33–35] but generally higher than that in suburban (8–60 ppb) and rural (13–23 ppb) areas in the PRD region.[33–37] It should be noted that the sampling was performed during the COVID-19 pandemic, which negatively affected the industrial activity. This might lead to the reduction in VOCs emission from the industrial park. These indicate that industrial emissions have a great impact on the regional atmospheric environment. In addition, complex emission sources would lead to an increase in the VOC levels and the levels of VOCs in urban areas with industrial parks were generally higher.

Based on the functional groups, the detected VOCs were classified as five categories namely alkanes (19 species), alkenes (8 species), aromatic hydrocarbons (AHs) (18 species), halogenated hydrocarbons (HHs) (33 species) and oxygenated VOCs (OVOCs) (3 species) (Table S2†). The concentrations of alkanes, alkenes, AHs, HHs and OVOCs were 14 ± 16, 6 ± 4, 10 ± 5, 9 ± 7 and 2 ± 2 ppb, respectively. Alkanes (35%) were the most contributing species, followed by AHs (24%), HHs (21%) and alkenes (14%), and the minimum contribution was from OVOCs (6%) (Fig. 2a).

Among these alkanes (Fig. 2b), undecane (27%), isopentane (23%), n-hexane (12%), 3-methylpentane (9%), and decane (4%)

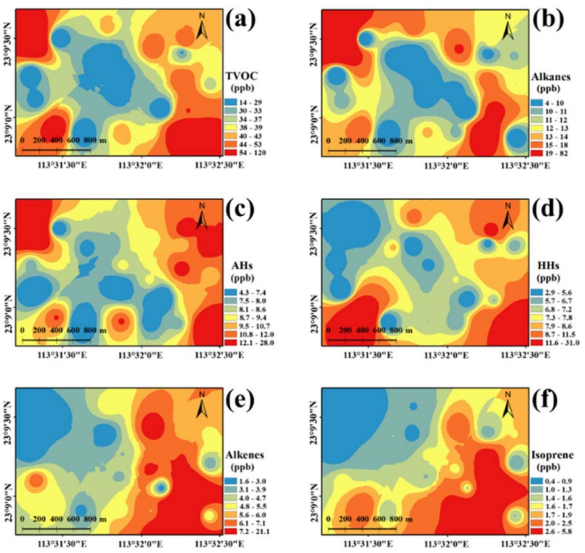

Fig. 1 The distribution of VOCs and air pollutants. The colours from blue to red represent a gradual increase in concentration. (a) The distribution of TVOCs; (b) the distribution of alkanes; (c) the distribution of AHs; (d) the distribution of HHs; (e) the distribution of alkenes; (f) the distribution of isoprene.

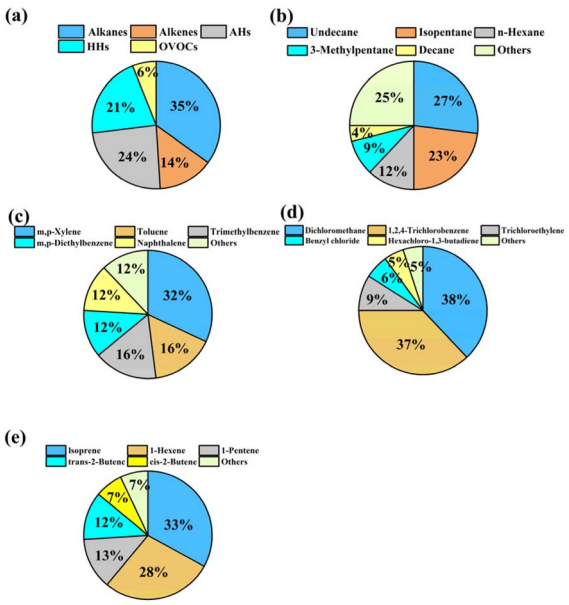

Fig. 2 The percentage of species and the contribution of dominant compounds: (a) the proportion of VOC species; (b) the ratio of the dominant species of alkanes; (c) the ratio of the dominant species of AHs; (d) the ratio of the dominant species of HHs; (e) the ratio of the dominant species of alkenes.

were the dominant species and their concentrations varied from 13 to 92 ppb. Furthermore, the spatial distribution of alkanes was illustrated (Fig. 1b). A high value (83 ppb) of alkanes was found in the northwestern region of the industrial park. It is worth noting that a highway toll station is located nearby, which might be the reason for the high concentration of alkanes in this area, since these alkanes (*e.g.*, undecane and isopentane) were frequently detected in the vehicle exhaust, tunnels or roadways.[35,36] In addition, relatively high values (22–35 ppb) of alkanes were also found in the southeastern area, which had transportation, pharmaceutical manufacturing and machinery manufacturing, producing abundant alkanes.[37]

Among AHs (Fig. 2c), toluene and *m*, *p*-xylene had a similar level of 36 ppb and they totally represented 32% of AHs. Naphthalene, *m*, *p*-diethylbenzene, and trimethylbenzene were the second most AHs, each of which accounted for 12% of AHs. The spatial distribution of AHs is shown in Fig. 1c, which shows a high value (27 ppb) of AHs in the northwestern region of the industrial park, and they mainly consisted of *m*, *p*-diethylbenzene and 1,2,3-trimethylbenzene. These AHs in the northwestern region of the industrial park might be released from vehicle exhaust[38] and the pharmaceutical industry.[39] In addition, a relatively high value (13–17 ppb) of AHs was observed in the eastern region, and toluene and *m*, *p*-xylene were primarily detected AH species. According to previous studies, they were common compounds from vehicle emission[38] and evaporative loss of solvents during various industrial processes.[40] In this study, in the eastern region of the industrial park, there are approximately five logistics companies with dense traffic, which were the main source of AHs.

Among HHs (Fig. 2d), dichloromethane (38%), 1,2,4-trichlorobenzene (9%), trichloroethylene (6%), (chloromethyl)-benzene (5%) and hexachloro-1,3-butadiene (5%) were the dominant HH species (Fig. 2d). High levels of HHs were distributed in the southeastern (31 ppb) and southwestern (31 ppb) regions of the industrial park (Fig. 1d). These regions were mostly affected by multiple pollution sources. HHs are mostly used as industrial solvents in certain sections of the pharmaceutical chemical industry[39] and chemical industry[41] (*e.g.*, coatings, fragrances and flavors, printing, textiles). Further, the contributions of solvent use, refrigeration and chemical manufacturing to HHs were remarkable in the PRD region,[42] Additionally, dichloromethane is mainly consumed in the pharmaceutical industry, metal cleaning agents and chemical production.[43] In the southwest and southeast regions of the study area, printing, textiles, raw material manufacturing, pharmaceutical manufacturing industries located here might be the main sources of HHs.

Among alkenes (Fig. 2e), the five dominant species were isoprene (33%), 1-hexene (28%), 1-pentene (13%), *trans*-2-butene (13%) and *cis*-2-butene (7%). The high-value (8–21 ppb) region of alkenes was distributed in the eastern region (Fig. 1e). Abundant isoprene was measured in the eastern region of the industrial park (Fig. 1f), which was adjacent to a mountain covered with plentiful trees. Therefore, isoprene in the eastern region was likely due to the vegetation emission in the mountain.

Comparatively, the measured VOCs were dominated by alkanes (42%), followed by aromatics (20%), alkenes (18%), and halo-hydrocarbons (13%) in a typical petrochemical area in the Yangtze River Delta, China.[44] The most dominant VOCs were alkanes (45%), followed by alkenes (25%) and AHs (22%) in an complicated industrial area of Nanjing, China.[34] That is, the contribution ratio of these species in this study varied from other industrial parks, but alkanes and AHs were mainly from industrial emission.

3.2. Characteristics of NO_X and O_3

NO_X and O_3 were simultaneously monitored at sampling sites in the industrial park. As shown in Fig. 3 and S4†, the average concentration of NO_X was 30 ± 10 ppb, ranging from 7 to 47 ppb. High levels (33–47 ppb) of NO_X appeared in the western region, which was close to a roadway. However, a different distribution between NO and NO_2 was found in the western region. A higher value of NO was measured in the northwestern region (19–21 ppb) compared to the southeastern region (5–8 ppb). The spatial distribution of NO_2 showed an opposite feature. Such an opposing feature of NO and NO_2 can be attributed to the efficient conversion NO to NO_2, as discussed below.

For the O_3, it can be found that the concentration of O_3 ranged from 36 to 85 ppb, with a mean value of 55 ± 16 ppb (Fig. S4†). Interestingly, high values of O_3 were found in the eastern and northern regions of the industrial park (Fig. 3d), where the level of NO_2 showed low values. In contrast, a low level of O_3 and a high concentration of NO_2 were observed in the southwestern or southeast region of the industrial park. This difference in spatial distribution between O_3, NO, and NO_2 suggests that the formation of O_3 in these regions was strongly related to the variation in the levels of NO and NO_2. However, relatively low values of O_3 and high values of VOCs were distributed in northeastern or southeastern regions in the industrial park, as previously discussed.

3.3. Formation of O_3 related to VOCs and NO_X

The contribution of precursors to the formation of O_3 can be described as from VOC-limited, NOx-limited or their transition regimes. A ratio of VOCs to NO_X has been widely employed to

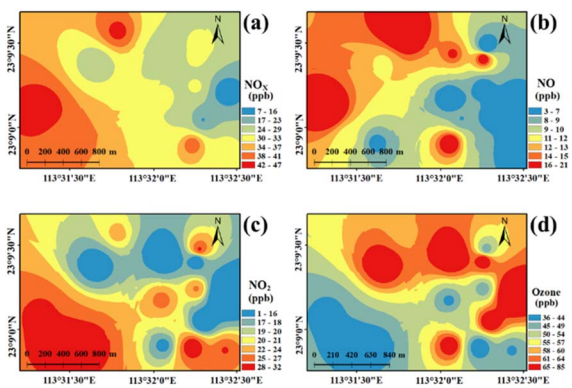

Fig. 3 The distributions of NOx and ozone. The colours from blue to red represent a gradual increase in concentration: (a) the distribution of NOx; (b) the distribution of NO; (c) the distribution of NO_2; (d) the distribution of ozone.

evaluate the sensitivity of O_3 formation to the VOC-limited or NO_X-limited regime in various studies.[45–47] In this study, the VOC/NO_X ratio varied from 0.5 to 5.7, with a mean value of 1.8. These VOC/NO_X ratios were much lower than the 8 : 1 threshold for a transition from the VOC-limited to the NOx-limited regime,[48,49] suggesting that the formation of O_3 in the industrial park was probably in the VOC-limited regime. It must be pointed out that these results exhibited here were on the basis of the threshold value of the VOC/NO_X ratio reported for Los Angeles.[50] Based on the observation-based chemical box model, the RIR values of NO_X and VOCs were −0.45 and 0.21, respectively, suggesting that the reduction of O_3 in the industrial park was VOC-sensitive. The RIR values of alkanes, alkenes (not including isoprene), isoprene, aromatic hydrocarbons, halogenated hydrocarbons and OVOCs were 0.01, 0.07, 0.06, 0.05, 0.01 and 0.01, respectively.

To further evaluate the formation of O_3 sensitive to VOCs in the industrial park, high (above 50 ppb) and low (below 50 ppb) concentrations of O_3 with change in concentration and species of VOCs were discussed. The concentration of TVOCs in the high O_3 region (35 ± 12 ppb) was comparable to that in the low O_3 region (48 ± 21 ppb) (Fig. 4a). Similar values of alkanes, alkenes, AHs and OVOCs in the industrial park were also found in the high and low O_3 regions (Fig. S5†). However, a lower level of HHs in the high O_3 region (14 ± 11 ppb) was measured compared to that in the low O_3 region (7 ± 2 ppb). Thus, the concentration of the generated O_3 is closely related to the concentration and species of VOCs.

Due to the difference in the reactivity of individual VOC species to generate O_3, the OFP of individual VOC species was also used to evaluate the contribution of VOCs to the generation of O_3 in the high and low O_3 regions in this study. As previously discussed, the increase in the reactive VOCs would result in the formation of O_3 due to the VOC-limited regime.[51,52] Fig. 5 shows the OFP values of reactive VOCs and their proportion. The maximum value of OFP for VOCs was contributed by alkenes (40%), followed by AHs (39%), alkanes (12%) and OVOCs (7%), and the minor contribution was from HHs (2%) (Fig. 5a). More specifically, isoprene, *trans*-2-butene and 1-hexene contributed to 36%, 20% and 16% of OFP, respectively, in the alkenes. *Cis*-2-butene and 1-pentene showed a similar proportion of 10% in the alkenes (Fig. 5b). Xylene and trimethylbenzene accounted for 30% and 23% of OFP in the AHs, respectively. Approximately 12% of OFP in the AHs was attributed to toluene (Fig. 5c).

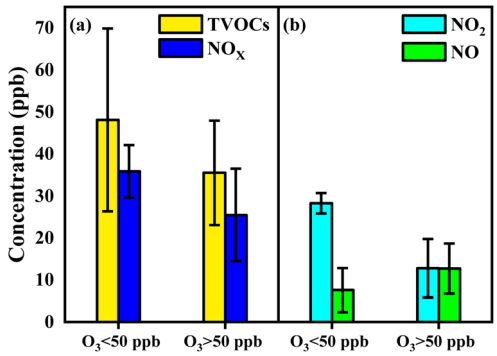

Fig. 4 (a) The concentration of TVOCs in the high O_3 region and the low O_3 region; (b) the concentration of NOx in the high O_3 region and the low O_3 region.

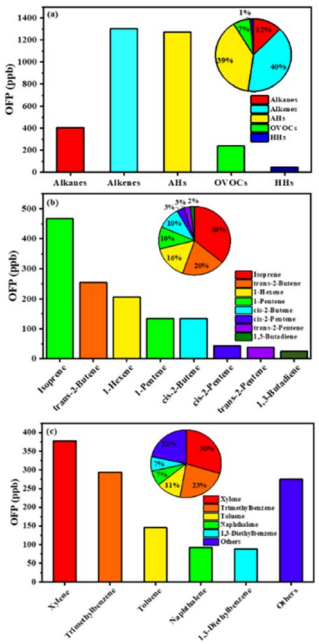

Fig. 5 The OFP values of reactive VOCs and their proportion. (a) VOC species; (b) the dominant species of alkenes; (c) the dominant species of AHs.

Further, the distribution of OFP values in the investigated industrial park was demonstrated. There was no increase in OFP values in the high O_3 region (132 ± 52 ppb) compared with the low O_3 region (153 ± 58 ppb) (Fig. S6†). Moreover, the spatial distribution of OFP showed that a high value of OFP appeared in the southeastern region of the industrial park (Fig. S7†), where existed a low value of O_3. These results imply that the enrichment of O_3 has not occurred in the high OFP value of VOCs.

The concentration of NOx in the high O_3 region was 25 ± 10 ppb, which was lower than 36 ± 6 ppb in the low O_3 region, as shown in Fig. 4b. This indicates that the formation of O_3 in the industrial park readily occurred in the low NOx region. In the meantime, a lower level of NO_2 (13 ± 7 ppb) was observed in the high O_3 region relative to that (28 ± 2 ppb) in the low O_3 region (Fig. 4b). In contrast, a higher level of NO (13 ± 5 ppb) in the high O_3 region was compared with that (8 ± 5 ppb) in the low O_3 region. This diversity suggests that O_3 is enriched in the low NO_2 region or high NO region in the industrial park.

The low O_3 region in the industrial park was mostly due to the titration reaction of NO and O_3 to form NO_2, in turn, showing high values of NO_2 in the low O_3 region.[53,54] This reaction also leads to the consumption of NO, therefore reducing NO in the low O_3 region. The reduction of O_3 in the high OFP value region in the industrial park can be attributed to the presence of the titration reaction, in spite of the production of O_3 in the VOC-limited regime. In contrast, abundant NO and the decrease in NO_2 in the high O_3 region relative to the low O_3

region suggest that the effect of the titration reaction on the consumption of O_3 was minor, therefore leading to the accumulation of O_3.

The mean concentration of O_3 was 55 ± 16 ppb in this study, which was higher than the averaged O_3 concentration of 35–50 ppb from 57 national monitoring sites in the PRD region.[55] Generally, higher averaged O_3 levels (about 20–60 ppb) in the suburban or rural sites were compared with those in the urban sites (about 10–45 ppb) in the PRD region.[56] The NO titration effect likely leads to the decrease in O_3 levels in urban sites,[55] which agreed with the finding in the current study. However, higher levels of O_3 in the industrial park relative to urban sites in the PRD region might be also related to meteorological conditions. Low wind and sunny day during the sampling period would also accumulate precursors and thus lead to O_3 formation in the small industrial park.

It was found that the VOC-limited region was mostly located at urban cores and large city clusters in the PRD region through the analysis of the whole PRD.[57,58] Lu *et al.* mentioned that the O_3 formation was in a VOC-limited regime in Guangzhou and Hong Kong, South China.[59] Several studies also showed that the formation of O_3 in urban sites of Guangzhou was mainly limited by VOCs.[60–62] Oppositely, the generation of O_3 in the NOx-limited or transition regime was observed in the suburban or rural sites of the PRD region.[58,63] For example, Wang *et al.* indicated that the formation of O_3 was frequent in the NOx-limited regime at a rural site in the PRD.[58] Wang *et al.* found differently that a rural site in Hong Kong was a transition regime.[64] Li *et al.* pointed out that the O_3 formation regime would change over complicated spatial and diurnal variations.[65]

In the present work, the O_3 formation was VOC-limited in the industrial park, which is in agreement with the findings at urban sites in the PRD region reported previously.[60,63] However, due to the variation in the reactivity or sources of VOCs among different urban or industrial sites, changes in VOCs would alter the contribution of VOCs to the production of O_3 at different sites. Louie *et al.* observed three sites in the PRD from 2008 to 2009, and found that AHs and alkenes together contributed to about 80% of the total OFP of VOCs, while alkanes contributed to 12%–14%.[66] Ou *et al.* also found that AHs and alkenes become predominant with contributions of 59% and 26%, respectively, of the total OFP.[67] Similar to our research, we found that AHs and alkenes made up 79% of the total OFP. Vehicle exhaust and industrial processes (*e.g.* pharmaceutical industry, raw material manufacturing, electronic and machine manufacturing) were the factors that mainly contributed to the OFP in PRD, making up more than 40% of the total OFP.[68] It is worth noting that even though the industrial park was in a VOC-limited regime, due to the different sources and compositions of VOCs, the targets for ozone reduction and control of VOCs are also different. In this park, vehicle exhaust and industrial processes mentioned above were the important control sources.

3.4. Atmospheric implication

Multi-site observation presented here found that abundant NOx (33–47 ppb) and TVOCs (71–120 ppb) in the western region of the industrial park were related to vehicle emissions. The enrichment of TVOCs (65–76 ppb) in the eastern region of the industrial park was likely attributed to the industrial emissions. Multi-site observation can provide a clearly spatial distribution of atmospheric pollution in a study area, which was a supplement to the measurement at an individual site. Our results also showed that the reduction in O_3 in the high OFP region was due to the consumption of O_3 *via* the titration reaction. Therefore, the multi-site observation will be a useful method to better understand the source and evolution of atmospheric pollution, especially in the small scale, such as an industrial park.

The O_3 abatement should be achieved by the reduction of its precursors. Our results suggest that O_3 formation in the industrial park was in the VOC-limited regime due to the ratios of VOCs/NO_X ranging from 0.5 to 5.7. Xylene (12%), trimethylbenzene (9%), and *trans*-2-butene (8%) emitted from vehicular or industrial emissions in the industrial park have been considered as the significant contributors to O_3 formation. Thus, reduction of these VOC emissions in the industrial park might be helpful for alleviating O_3 pollution.

Although it showed high OFP values for the O_3 formation, the stronger titration reaction led to a significant decrease in O_3. The NO_X concentration changed from 25 ± 10 to 36 ± 6 ppb, corresponding to the high O_3 region and low O_3 region in the industrial park, respectively. Several studies also observed that reducing a small amount of NOx in the PRD region would lead to an increase in O_3 concentration in the VOC-limited regime, and it was called as the NOx titration trap.[65,69] Such a NOx emission reduction was counterproductive for reducing VOC-limited O_3 concentrations only if the reduction of NOx was large enough or the emission of VOC was eliminated altogether.[70] Tang *et al.* found that Beijing successfully bypassed the NOx titration trap *via* elimination of scattered emission sources as well as the implementation of the China National VI (A) standard for motor vehicles after 2016.[71] Therefore, these control strategies might not only result in the decrease of VOC emission, but also reduction of NOx emission in the PRD region, while, bypassing the NOx titration trap in the future.

4 Conclusions

The simultaneous measurements of VOCs, NO_X and O_3 were conducted at multi-sample sites in an industrial park of the PRD region. The ratio of VOCs to NO_X ranging from 0.5 to 5.7 indicates that the formation of O_3 was in the VOC-limited regime in the industrial park. Alkenes and AHs principally from motor vehicles and industrial sources have been considered as the main potential contributors to the formation of O_3 in the industrial park. However, no increase in O_3 was found in the abundant alkene and AH regions, which showed high NO_2 or low NO values in the industrial park. This was mostly due to the titration reaction of NO and O_3 to form NO_2, therefore leading to the consumption of O_3. These findings highlighted the role of NOx-titration in the formation of O_3 under the VOC-limited regime. Thus, the policy for O_3 abatement in the study region might consider the control of VOC emission as well as NO_X-titration.

Data availability

The data supporting this article have been included as part of the ESI.†

Author contributions

Taicheng An: conceptualization, writing–review & editing, supervision, funding acquisition. Jiajia Li: investigation, methodology, data curation. Qinhao Lin: methodology, investigation. Guiying Li: writing–review & editing, data curation.

Conflicts of interest

There are no conflicts to declare.

Acknowledgements

This work was supported by the National Natural Science Foundation of China (42327806, 42020104001, and 42277398), Local Innovative and Research Teams Project of Guangdong Pearl River Talents Program (2017BT01Z032), Natural Science Foundation of Guangdong Province (2023A1515030186 and 2021A1515011492), and Science and Technology Program of Guangzhou (2024A04J9881).

Notes and references

1 A. Pandey, M. Brauer, M. L. Cropper, K. Balakrishnan, P. Mathur, S. Dey, B. Turkgulu, G. A. Kumar, M. Khare, G. Beig, T. Gupta, R. P. Krishnankutty, K. Causey, A. J. Cohen, S. Bhargava, A. N. Aggarwal, A. Agrawal, S. Awasthi, F. Bennitt, S. Bhagwat, P. Bhanumati, K. Burkart, J. K. Chakma, T. C. Chiles, S. Chowdhury, D. J. Christopher, S. Dey, S. Fisher, B. Fraumeni, R. Fuller, A. G. Ghoshal, M. J. Golechha, P. C. Gupta, R. Gupta, R. Gupta, S. Gupta, S. Guttikunda, D. Hanrahan, S. Harikrishnan, P. Jeemon, T. K. Joshi, R. Kant, S. Kant, T. Kaur, P. A. Koul, P. Kumar, R. Kumar, S. L. Larson, R. Lodha, K. K. Madhipatla, P. A. Mahesh, R. Malhotra, S. Managi, K. Martin, M. Mathai, J. L. Mathew, R. Mehrotra, B. V. M. Mohan, V. Mohan, S. Mukhopadhyay, P. Mutreja, N. Naik, S. Nair, J. D. Pandian, P. Pant, A. Perianayagam, D. Prabhakaran, P. Prabhakaran, G. K. Rath, S. Ravi, A. Roy, Y. D. Sabde, S. Salvi, S. Sambandam, B. Sharma, M. Sharma, S. Sharma, R. S. Sharma, A. Shrivastava, S. Singh, V. Singh, R. Smith, J. D. Stanaway, G. Taghian, N. Tandon, J. S. Thakur, N. J. Thomas, G. S. Toteja, C. M. Varghese, C. Venkataraman, K. N. Venugopal, K. D. Walker, A. Y. Watson, S. Wozniak, D. Xavier, G. N. Yadama, G. Yadav, D. K. Shukla, H. J. Bekedam, K. S. Reddy, R. Guleria, T. Vos, S. S. Lim, R. Dandona, S. Kumar, P. Kumar, P. J. Landrigan and L. Dandona, Health and economic impact of air pollution in the states of India: the Global Burden of Disease Study 2019, *Lancet Planet. Health*, 2021, **5**, e25–e38.

2 J. Tirado, A. O. Torti, B. J. Butterworth, K. Wangen, A. Voon, B. Kies, J. P. Hupy, G. de Boer, R. B. Pierce, T. J. Wagner and P. A. Cleary, Observations of coastal dynamics during lake breeze at a shoreline impacted by high ozone, *Environ. Sci.: Atmos.*, 2023, **3**, 494–505.

3 L. Emberson, Effects of ozone on agriculture, forests and grasslands, *Philos. Trans. R. Soc., A*, 2020, **378**, 20190327.

4 J. Cao, X. Wang, H. Zhao, M. Ma and M. Chang, Evaluating the effects of ground-level O_3 on rice yield and economic losses in Southern China, *Environ. Pollut.*, 2020, **267**, 115694.

5 M. Takahashi, Z. Feng, T. A. Mikhailova, O. V. Kalugina, O. V. Shergina, L. V. Afanasieva, R. K. J. Heng, N. M. A. Majid and H. Sase, Air pollution monitoring and tree and forest decline in East Asia: A review, *Sci. Total Environ.*, 2020, **742**, 140288.

6 M. Aghapour, N. D. Ubags, D. Bruder, P. S. Hiemstra, V. Sidhaye, F. Rezaee and I. H. Heijink, Role of air pollutants in airway epithelial barrier dysfunction in asthma and COPD, *Eur. Respir. Rev.*, 2022, **31**, 210112.

7 K. Fan, N. Dong, M. Fang, Z. Xiang, L. Zheng, M. Wang, Y. Shi, G. Tan, C. Li and Y. Xue, Ozone exposure affects corneal epithelial fate by promoting mtDNA leakage and cGAS/STING activation, *J. Hazard. Mater.*, 2024, **465**, 133219.

8 R. Abolhasani, F. Araghi, M. Tabary, A. Aryannejad, B. Mashinchi and R. M. Robati, The impact of air pollution on skin and related disorders: A comprehensive review, *Dermatol. Ther.*, 2021, **34**, e14840.

9 H. Luo, J. Chen, G. Li and T. An, Formation kinetics and mechanisms of ozone and secondary organic aerosols from photochemical oxidation of different aromatic hydrocarbons: dependence on NOx and organic substituents, *Atmos. Chem. Phys.*, 2021, **21**, 7567–7578.

10 X. Zhou, X. Zhou, C. Wang and H. Zhou, Environmental and human health impacts of volatile organic compounds: A perspective review, *Chemosphere*, 2023, **313**, 137489.

11 H. Fan, C. Zhao and Y. Yang, A comprehensive analysis of the spatio-temporal variation of urban air pollution in China during 2014-2018, *Atmos. Environ.*, 2020, **220**, 117066.

12 F. Shen, L. Zhang, L. Jiang, M. Tang, X. Gai, M. Chen and X. Ge, Temporal variations of six ambient criteria air pollutants from 2015 to 2018, their spatial distributions, health risks and relationships with socioeconomic factors during 2018 in China, *Environ. Int.*, 2020, **137**, 105556.

13 L. K. Whalley, E. J. Slater, R. Woodward-Massey, C. Ye, J. D. Lee, F. Squires, J. R. Hopkins, R. E. Dunmore, M. Shaw, J. F. Hamilton, A. C. Lewis, A. Mehra, S. D. Worrall, A. Bacak, T. J. Bannan, H. Coe, C. J. Percival, B. Ouyang, R. L. Jones, L. R. Crilley, L. J. Kramer, W. J. Bloss, T. Vu, S. Kotthaus, S. Grimmond, Y. Sun, W. Xu, S. Yue, L. Ren, W. J. F. Acton, C. N. Hewitt, X. Wang, P. Fu and D. E. Heard, Evaluating the sensitivity of radical chemistry and ozone formation to ambient VOCs and NOx in Beijing, *Atmos. Chem. Phys.*, 2021, **21**, 2125–2147.

14 Y. Li, S. Yin, S. Yu, L. Bai, X. Wang, X. Lu and S. Ma, Characteristics of ozone pollution and the sensitivity to precursors during early summer in central plain, China, *J. Environ. Sci.*, 2021, **99**, 354–368.

15 S. Han, Q. Yao, X. Tie, Y. Zhang, M. Zhang, P. Li and Z. Cai, Analysis of surface and vertical measurements of O_3 and its chemical production in the NCP region, China, *Atmos. Environ.*, 2020, **241**, 117759.
16 P. Wang, Y. Chen, J. Hu, H. Zhang and Q. Ying, Attribution of tropospheric ozone to NOx and VOC emissions: considering ozone formation in the transition regime, *Environ. Sci. Technol.*, 2019, **53**, 1404–1412.
17 J. Feldner, M. O. P. Ramacher, M. Karl, M. Quante and M. L. Luttkus, Analysis of the effect of abiotic stressors on BVOC emissions from urban green infrastructure in northern Germany, *Environ. Sci.: Atmos.*, 2022, **2**, 1132–1151.
18 K. R. Hakeem, M. Sabir, M. Ozturk, M. S. Akhtar and F. H. Ibrahim, in *Reviews of Environmental Contamination and Toxicology*, ed. P. de Voogt, Springer International Publishing, Cham, 2017, vol. 242, pp. 183–217, DOI: 10.1007/398_2016_11.
19 M. Mayer, S. F. Schreier, W. Spangl, C. Staehle, H. Trimmel and H. E. Rieder, An analysis of 30 years of surface ozone concentrations in Austria: temporal evolution, changes in precursor emissions and chemical regimes, temperature dependence, and lessons for the future, *Environ. Sci.: Atmos.*, 2022, **2**, 601–615.
20 M. Song, X. Li, S. Yang, X. Yu, S. Zhou, Y. Yang, S. Chen, H. Dong, K. Liao, Q. Chen, K. Lu, N. Zhang, J. Cao, L. Zeng and Y. Zhang, Spatiotemporal variation, sources, and secondary transformation potential of volatile organic compounds in Xi'an, China, *Atmos. Chem. Phys.*, 2021, **21**, 4939–4958.
21 M. Li, Z. Klimont, Q. Zhang, R. V. Martin, B. Zheng, C. Heyes, J. Cofala, Y. Zhang and K. He, Comparison and evaluation of anthropogenic emissions of SO_2 and NO_x over China, *Atmos. Chem. Phys.*, 2018, **18**, 3433–3456.
22 C. Q. He, Y. Zou, S. J. Lv, R. M. Flores, X. L. Yan, T. Deng and X. J. Deng, The importance of photochemical loss to source analysis and ozone formation potential: Implications from in-situ observations of volatile organic compounds (VOCs) in Guangzhou, China, *Atmos. Environ.*, 2024, **320**, 120320.
23 W. Zhao, B. Gao, Q. Lu, Z. Zhong, X. Liang, M. Liu, S. Ma, J. Sun, L. Chen and S. Fan, Ozone Pollution Trend in the Pearl River Delta Region During 2006-2019, *Environ. Scic.*, 2021, **42**, 97–105.
24 L. Ye, X. Wang, S. Fan, W. Chen, M. Chang, S. Zhou, Z. Wu and Q. Fan, Photochemical indicators of ozone sensitivity: application in the Pearl River Delta, China, *Front. Environ. Sci. Eng.*, 2016, **10**, 15.
25 Q. Lu, J. Zheng, S. Ye, X. Shen, Z. Yuan and S. Yin, Emission trends and source characteristics of SO_2, NOx, PM_{10} and VOCs in the Pearl River Delta region from 2000 to 2009, *Atmos. Environ.*, 2013, **76**, 11–20.
26 Y. Bian, Z. Huang, J. Ou, Z. Zhong, Y. Xu, Z. Zhang, X. Xiao, X. Ye, Y. Wu, X. Yin, C. Li, L. Chen, M. Shao and J. Zheng, Evolution of anthropogenic air pollutant emissions in Guangdong Province, China, from 2006 to 2015, *Atmos. Chem. Phys.*, 2019, **19**, 11701–11719.
27 C.-H. Chen, Y.-C. Chuang, C.-C. Hsieh and C.-S. Lee, VOC characteristics and source apportionment at a PAMS site near an industrial complex in central Taiwan, *Atmos. Pollut. Res.*, 2019, **10**, 1060–1074.
28 G. F. Chen, C. H. Lai and W. H. Chen, Principal Component Analysis and Mapping to Characterize the Emission of Volatile Organic Compounds in a Typical Petrochemical Industrial Park, *Aerosol Air Qual. Res.*, 2020, **20**, 465–476.
29 L. Bai, X. Lu, S. Yin, H. Zhang, S. Ma, C. Wang, Y. Li and R. Zhang, A recent emission inventory of multiple air pollutant, $PM_{2.5}$ chemical species and its spatial-temporal characteristics in central China, *J. Cleaner Prod.*, 2020, **269**, 122114.
30 X. Pang, L. Chen, K. Shi, F. Wu, J. Chen, S. Fang, J. Wang and M. Xu, A lightweight low-cost and multipollutant sensor package for aerial observations of air pollutants in atmospheric boundary layer, *Sci. Total Environ.*, 2021, **764**, 142828.
31 M. Marty, F. Spurlock and T. Barry, in *Hayes' Handbook of Pesticide Toxicology*, ed. R. Krieger, Academic Press, New York, 3rd edn, 2010, pp. 571–585, DOI: 10.1016/B978-0-12-374367-1.00019-7.
32 M. A. Venecek, W. P. L. Carter and M. J. Kleeman, Updating the SAPRC Maximum Incremental Reactivity (MIR) scale for the United States from 1988 to 2010, *J. Air Waste Manage. Assoc.*, 2018, **68**, 1301–1316.
33 C. Han, R. Liu, H. Luo, G. Li, S. Ma, J. Chen and T. An, Pollution profiles of volatile organic compounds from different urban functional areas in Guangzhou China based on GC/MS and PTR-TOF-MS: atmospheric environmental implications, *Atmos. Environ.*, 2019, **214**, 116843.
34 J. An, B. Zhu, H. Wang, Y. Li, X. Lin and H. Yang, Characteristics and source apportionment of VOCs measured in an industrial area of Nanjing, Yangtze River Delta, China, *Atmos. Environ.*, 2014, **97**, 206–214.
35 L. Benbrahim-Tallaa, R. A. Baan, Y. Grosse, B. Lauby-Secretan, F. El Ghissassi, V. Bouvard, N. Guha, D. Loomis and K. Straif, Carcinogenicity of diesel-engine and gasoline-engine exhausts and some nitroarenes, *Lancet Oncol.*, 2012, **13**, 663–664.
36 Y. Wang, G. Yang, L. Wang, L. Zhao, S. Ji, M. Qi, X. Lu, Z. Liu, J. Tan, Y. Liu, Q. Wang and R. Xu, Characteristics and Source Apportionment of VOCs in a City with Complex Pollution in China, *Aerosol Air Qual. Res.*, 2020, **20**, 2196–2210.
37 Z. Zhou, Q. Tan, Y. Deng, C. Lu, D. Song, X. Zhou, X. Zhang and X. Jiang, Source profiles and reactivity of volatile organic compounds from anthropogenic sources of a megacity in southwest China, *Sci. Total Environ.*, 2021, **790**, 148149.
38 S. Xiao, Y. Zhang, Z. Zhang, W. Song, C. Pei, D. Chen and X. Wang, The contributions of non-methane hydrocarbon emissions by different fuel type on-road vehicles based on tests in a heavily trafficked urban tunnel, *Sci. Total Environ.*, 2023, **873**, 162432.
39 N. Cheng, D. Jing, C. Zhang, Z. Chen, W. Li, S. Li and Q. Wang, Process-based VOCs source profiles and contributions to ozone formation and carcinogenic risk in a typical chemical synthesis pharmaceutical industry in China, *Sci. Total Environ.*, 2021, **752**, 141899.

40 X. Lu, D. Gao, Y. Liu, S. Wang, Q. Lu, S. Yin, R. Zhang and S. Wang, A recent high-resolution PM2.5 and VOCs speciated emission inventory from anthropogenic sources: A case study of central China, *J. Cleaner Prod.*, 2023, **386**, 135795.

41 P. Zheng, T. Chen, C. Dong, Y. Liu, H. Li, G. Han, J. Sun, L. Wu, X. Gao, X. Wang, Y. Qi, Q. Zhang, W. Wang and L. Xue, Characteristics and sources of halogenated hydrocarbons in the Yellow River Delta region, northern China, *Atmos. Res.*, 2019, **225**, 70–80.

42 H. Guo, A. J. Ding, T. Wang, I. J. Simpson, D. R. Blake, B. Barletta, S. Meinardi, F. S. Rowland, S. M. Saunders, T. M. Fu, W. T. Hung and Y. S. Li, Source origins, modeled profiles, and apportionments of halogenated hydrocarbons in the greater Pearl River Delta region, southern China, *J. Geophys. Res.: Atmos.*, 2009, **114**, 11448.

43 N. Yang, in *Encyclopedia of Toxicology*, ed. P. Wexler, Academic Press, Oxford, 3rd edn, 2014, pp. 99–101, DOI: 10.1016/B978-0-12-386454-3.01218-5.

44 Y. Zhang, R. Li, H. Fu, D. Zhou and J. Chen, Observation and analysis of atmospheric volatile organic compounds in a typical petrochemical area in Yangtze River Delta, China, *J. Environ. Sci.*, 2018, **71**, 233–248.

45 K. Bali, A. Kumar and S. Chourasiya, Emission estimates of trace gases (VOCs and NOx) and their reactivity during biomass burning period (2003-2017) over Northeast India, *J. Atmos. Chem.*, 2021, **78**, 17–34.

46 Y. Zou, X. J. Deng, D. Zhu, D. C. Gong, H. Wang, F. Li, H. B. Tan, T. Deng, B. R. Mai, X. T. Liu and B. G. Wang, Characteristics of 1 year of observational data of VOCs, NO_x and O_3 at a suburban site in Guangzhou, China, *Atmos. Chem. Phys.*, 2015, **15**, 6625–6636.

47 Z. Tan, K. Lu, M. Jiang, R. Su, H. Dong, L. Zeng, S. Xie, Q. Tan and Y. Zhang, Exploring ozone pollution in Chengdu, southwestern China: A case study from radical chemistry to O_3-VOC-NOx sensitivity, *Sci. Total Environ.*, 2018, **636**, 775–786.

48 B. Liu, D. Liang, J. Yang, Q. Dai, X. Bi, Y. Feng, J. Yuan, Z. Xiao, Y. Zhang and H. Xu, Characterization and source apportionment of volatile organic compounds based on 1-year of observational data in Tianjin, China, *Environ. Pollut.*, 2016, **218**, 757–769.

49 S. Fu, M. Guo, J. Luo, D. Han, X. Chen, H. Jia, X. Jin, H. Liao, X. Wang, L. Fan and J. Cheng, Improving VOCs control strategies based on source characteristics and chemical reactivity in a typical coastal city of South China through measurement and emission inventory, *Sci. Total Environ.*, 2020, **744**, 140825.

50 J. H. Seinfeld, Urban air pollution: state of the science, *Science*, 1989, **243**, 745–752.

51 K. Zhang, L. Li, L. Huang, Y. Wang, J. Huo, Y. Duan, Y. Wang and Q. Fu, The impact of volatile organic compounds on ozone formation in the suburban area of Shanghai, *Atmos. Environ.*, 2020, **232**, 117511.

52 Y. Zhang, L. Xue, W. P. L. Carter, C. Pei, T. Chen, J. Mu, Y. Wang, Q. Zhang and W. Wang, Development of ozone reactivity scales for volatile organic compounds in a Chinese megacity, *Atmos. Chem. Phys.*, 2021, **21**, 11053–11068.

53 S. Han, Analysis of the Relationship between O_3, NO and NO_2 in Tianjin, China, *Aerosol Air Qual. Res.*, 2011, **11**, 128–139.

54 A. L. Londhe, D. B. Jadhav, P. S. Buchunde and M. J. Kartha, Surface ozone variability in the urban and nearby rural locations of tropical India, *Curr. Sci.*, 2008, **95**, 1724–1729.

55 J. F. Li, K. D. Lu, W. Lv, J. Li, L. J. Zhong, Y. B. Ou, D. H. Chen, X. Huang and Y. H. Zhang, Fast increasing of surface ozone concentrations in Pearl River Delta characterized by a regional air quality monitoring network during 2006-2011, *J. Environ. Sci.*, 2014, **26**, 23–36.

56 X. B. Li, B. Yuan, D. D. Parrish, D. H. Chen, Y. X. Song, S. X. Yang, Z. J. Liu and M. Shao, Long-term trend of ozone in southern China reveals future mitigation strategy for air pollution, *Atmos. Environ.*, 2022, **269**, 118869.

57 P. Wang, Y. Chen, J. L. Hu, H. L. Zhang and Q. Ying, Source apportionment of summertime ozone in China using a source-oriented chemical transport model, *Atmos. Environ.*, 2019, **211**, 79–90.

58 X. Wang, Y. Zhang, Y. Hu, W. Zhou, K. Lu, L. Zhong, L. Zeng, M. Shao, M. Hu and A. G. Russell, Process analysis and sensitivity study of regional ozone formation over the Pearl River Delta, China, during the PRIDE-PRD2004 campaign using the Community Multiscale Air Quality modeling system, *Atmos. Chem. Phys.*, 2010, **10**, 4423–4437.

59 H. Lu, X. Lyu, H. Cheng, Z. Ling and H. Guo, Overview on the spatial-temporal characteristics of the ozone formation regime in China, *Environ. Sci.: Processes Impacts*, 2019, **21**, 916–929.

60 M. Shao, Y. Zhang, L. Zeng, X. Tang, J. Zhang, L. Zhong and B. Wang, Ground-level ozone in the Pearl River Delta and the roles of VOC and NOx in its production, *J. Environ. Manage.*, 2009, **90**, 512–518.

61 H. Cheng, H. Guo, X. Wang, S. M. Saunders, S. H. Lam, F. Jiang, T. Wang, A. Ding, S. Lee and K. F. Ho, On the relationship between ozone and its precursors in the Pearl River Delta: application of an observation-based model (OBM), *Environ. Sci. Pollut. Res.*, 2010, **17**, 547–560.

62 L. K. Xue, T. Wang, J. Gao, A. J. Ding, X. H. Zhou, D. R. Blake, X. F. Wang, S. M. Saunders, S. J. Fan, H. C. Zuo, Q. Z. Zhang and W. X. Wang, Ground-level ozone in four Chinese cities: precursors, regional transport and heterogeneous processes, *Atmos. Chem. Phys.*, 2014, **14**, 13175–13188.

63 J. M. Ou, Z. B. Yuan, J. Y. Zheng, Z. J. Huang, M. Shao, Z. K. Li, X. B. Huang, H. Guo and P. K. K. Louie, Ambient Ozone Control in a Photochemically Active Region: Short Term Despiking or Long-Term Attainment?, *Environ. Sci. Technol.*, 2016, **50**, 5720–5728.

64 Y. Wang, H. Guo, S. Zou, X. Lyu, Z. Ling, H. Cheng and Y. Zeren, Surface O_3 photochemistry over the South China Sea: Application of a near-explicit chemical mechanism box model, *Environ. Pollut.*, 2018, **234**, 155–166.

65 Y. Li, A. K. H. Lau, J. C. H. Fung, J. Zheng and S. Liu, Importance of NOx control for peak ozone reduction in the

Pearl River Delta region, *J. Geophys. Res.: Atmos.*, 2013, **118**, 9428–9443.

66 P. K. K. Louie, J. W. K. Ho, R. C. W. Tsang, D. R. Blake, A. K. H. Lau, J. Z. Yu, Z. Yuan, X. Wang, M. Shao and L. Zhong, VOCs and OVOCs distribution and control policy implications in Pearl River Delta region, China, *Atmos. Environ.*, 2013, **76**, 125–135.

67 J. Ou, J. Zheng, R. Li, X. Huang, Z. Zhong, L. Zhong and H. Lin, Speciated OVOC and VOC emission inventories and their implications for reactivity-based ozone control strategy in the Pearl River Delta region, China, *Sci. Total Environ.*, 2015, **530–531**, 393–402.

68 R. Wu and S. Xie, Spatial Distribution of Ozone Formation in China Derived from Emissions of Speciated Volatile Organic Compounds, *Environ. Sci. Technol.*, 2017, **51**, 2574–2583.

69 M. Kang, J. Zhang, H. Zhang and Q. Ying, On the Relevancy of Observed Ozone Increase during COVID-19 Lockdown to Summertime Ozone and $PM_{2.5}$ Control Policies in China, *Environ. Sci. Technol. Lett.*, 2021, **8**, 289–294.

70 C. L. Blanchard, S. Tanenbaum and D. R. Lawson, Differences between Weekday and Weekend Air Pollutant Levels in Atlanta; Baltimore; Chicago; Dallas-Fort Worth; Denver; Houston; New York; Phoenix; Washington, DC; and Surrounding Areas, *J. Air Waste Manage. Assoc.*, 2008, **58**, 1598–1615.

71 G. Tang, Y. Liu, J. Zhang, B. Liu, Q. Li, J. Sun, Y. Wang, Y. Xuan, Y. Li, J. Pan, X. Li and Y. Wang, Bypassing the NOx titration trap in ozone pollution control in Beijing, *Atmos. Res.*, 2021, **249**, 105333.